



# Biological Macromolecule Composite Films Made from Sagu Starch and Flour/Poly( $\epsilon$ -Caprolactone) Blends Processed by Blending/Thermo Molding

Tomy J. Gutiérrez<sup>1</sup>

© Springer Science+Business Media, LLC, part of Springer Nature 2018

## Abstract

Non-conventional starch sources (starch and flour) obtained from sagu (*Canna edulis* Kerr) rhizomes grown in the Venezuelan Amazon were used as biological macromolecule matrices. Biological macromolecule composite films prepared from sagu starch and flour/poly( $\epsilon$ -caprolactone) (PCL) blends were then obtained by blending/thermo molding. The use of flours as a rich source of starch has attracted much attention as they are cheaper than starch, thus making them commercially more competitive. The PCL-containing films proved to be less stable in an alkaline medium and less dense (0.60–0.66 g/cm<sup>3</sup>), and were also thinner (1.15–1.17 mm), rougher, more crystalline (20.5–27.1%) and opaque (1.45–1.52) than the films without added PCL. Films made from the flour/PCL blend showed a greater phase separation than the starch/PCL films. The use of flour as a starchy source is interesting. However, the results of attenuated total reflectance Fourier transform infrared spectroscopy and water activity suggest that the films prepared from sagu starch-glycerol had stronger hydrogen bonding interactions than those made from flour-glycerol. This led to the sagu starch-based film being less susceptible to moisture and more stable under alkaline conditions.

**Keywords** Biological macromolecules · Microstructure · Non-conventional starches · Physicochemical properties · Polymer composites

## Introduction

The manufacture of starch-based films is an important component in the development of environmentally friendly materials as an alternative to those obtained from petroleum, this latter being one of the largest contributors to global pollution on the planet [1]. However, the high water sensitivity (hydrophilic nature) of starch films has limited their applications

[2]. To overcome this, several authors have proposed blending starch and other biodegradable polymers with hydrophobic characteristics such as poly( $\epsilon$ -caprolactone) (PCL) and polylactic acid (PLA), among others [3]. PCL is a semicrystalline biopolymer with a low glass transition temperature ( $\sim 60^\circ\text{C}$ ) and melting point (around  $59^\circ\text{C}$ ) [4, 5]. Nonetheless, starch/PCL blends are immiscible thus leading to phase separation [6]. Recently our research group has shown that mixing non-conventional sagu starch (*Canna edulis* Kerr), obtained from rhizomes grown in the Venezuelan Amazon, with PCL produces a more compatible blend than sagu flour/PCL [7]. This is unfortunate since sagu flour has a higher yield than the starch, and is also cheaper, thus making it more cost effective and hence more likely to displace the synthetic polymers in the market [7]. In spite of this, a more in-depth analysis of these materials is interesting at the scientific level, since research into processes such as blending followed by thermo molding for the production of starch films is scarce in the literature compared to methods such as casting. This latter is perfectly adequate on a laboratory scale. At an industrial level, however, it is not feasible as

**Electronic supplementary material** The online version of this article (<https://doi.org/10.1007/s10924-018-1268-6>) contains supplementary material, which is available to authorized users.

✉ Tomy J. Gutiérrez  
tomy.gutierrez@fi.mdp.edu.ar; tomy\_gutierrez@yahoo.es

<sup>1</sup> Grupo de Materiales Compuestos Termoplásticos (CoMP), Instituto de Investigaciones en Ciencia y Tecnología de Materiales (INTEMA), Facultad de Ingeniería, Universidad Nacional de Mar del Plata (UNMDP) y Consejo Nacional de Investigaciones Científicas y Técnicas (CONICET), B7608FLC, Colón 10850, Mar del Plata, Buenos Aires, Argentina

it consumes a great deal of energy during solvent (water) evaporation [8], thus impeding the manufacture of green materials with a low carbon footprint. For this reason, more studies into processing techniques that may be efficient at the industrial level should be undertaken, preferably those that could be applied using existing machines for processing polymers and/or biological macromolecules. One of these processes is blending followed by thermo molding, which was the focus of this study.

The aim of this research was thus to (1) analyze the structural and physicochemical properties; and (2) characterize the surface morphology of biological macromolecule composite films made from sagu starch/PCL and flour/PCL blends processed by blending/thermo molding.

## Experimental

### Materials

Native starch and flour obtained from sagu (*Canna edulis* Kerr) rhizomes grown in the Venezuelan Amazon were used as biological macromolecules for the development of composite films. Sagu starch was isolated by the protocol described by Pérez et al. [9] and the sagu flour was obtained using the methodology proposed by Pacheco [10]. Both these biological macromolecule matrices have already been characterized by our research group elsewhere (see Appendix A in Supplementary material, proximal analysis) [7]. Poly( $\epsilon$ -caprolactone) (PCL), molar weight 42,500 g/mol, was supplied by Aldrich Chemistry. Glycerol was purchased from Aurum, Argentina and employed as a plasticizer in the formation of the films.

### Film Formation

Biological macromolecule composite films prepared from sagu starch and flour were developed at a 1:1.4 (w/w) (glycerol/matrix) ratio, i.e. 9.5 g of glycerol and 12.5 g of matrix. The PCL-containing films were prepared by replacing 60% of the carbohydrate polymer matrices by PCL whilst maintaining the same percentage of glycerol. This, based on the best formula obtained in previous studies done by Mollega [11] and Maliger and Halley [12]. The films were processed by blending followed by thermo molding as follows: in each case the composite blends were pre-blended in a beaker. They were then introduced into a Brabender type mixer and blended at 130 °C and 60 rpm for 30 min. The resulting pastes were spread onto steel sheets and preheated for 5 min at 130 °C. They were then thermo molded at 130 °C for 15 min at 100 bars, before applying a cooling cycle until reaching a temperature of 30 °C. The resulting thermoplastic starch (TPS) and thermoplastic flour (TPF) films: native

sagu starch (TPS-NSS), native sagu starch/PCL blend (TPS-NSS/PCL), native sagu flour (TPF-NSF) and native sagu flour/PCL blend (TPF-NSF/PCL) were conditioned at ~57% relative humidity (RH) and 25 °C for a week before their characterization.

## Film Characterization

### Attenuated Total Reflectance Fourier Transform Infrared Spectroscopy (ATR/FTIR)

The IR spectra of the film samples were determined using a Nicolet 8700 infrared spectrometer (FTIR) from Thermo Scientific Instrument Corporation (Madison, Wisconsin, USA), equipped with a diamond at an incident angle of 45°. The spectra were recorded in Attenuated Total Reflectance mode (ATR) between 700 and 4000  $\text{cm}^{-1}$ , from 40 scans at a resolution of 4  $\text{cm}^{-1}$ . Each sample was scanned three times, observing good reproducibility.

### Determination of Film Thickness (e)

Film thickness ( $e$ ) was determined using a digital micrometer (Micromaster®) with an accuracy of  $\pm 0.001$  mm. Measurements were taken at eighteen random positions, and the results reported as mean values  $\pm$  standard deviation (SD).

### Density ( $\rho$ )

Film density was determined by cutting samples of each film into 20  $\times$  20 mm squares and measuring the thickness of each square at eighteen random positions. The samples were dried at 105 °C for 24 h and then weighed, and the density was calculated as the ratio between the weight and volume (thickness  $\times$  area) of each sample, using the following Eq. (1):

$$\rho = \frac{W_i - W_f}{l * w * e} \quad (1)$$

where  $W_i$  is the initial weight,  $W_f$  the final dry weight,  $l$  the length,  $w$  the width and  $e$  the thickness.

Density measurements were accomplished in triplicate, and the data reported as mean values  $\pm$  SD.

### Water Activity ( $a_w$ )

A psychrometric  $a_w$  meter Aqualab Cx-2 (Decagon Devices, Pullman, USA) previously calibrated with water at 25 °C was used to determine the water activity ( $a_w$ ) of the films. Three measurements were taken for each film and the average value  $\pm$  SD was reported.

## Stability in Acidic or Alkaline Solutions

In order to estimate the stability of the films in acidic and alkaline solutions, 12 mm diameter discs were immersed in containers with 20 mL of standard solutions of hydrochloric acid (0.1 mol/L = pH 1) or sodium hydroxide (0.1 mol/L = pH 13). The containers were sealed and maintained at 25 °C for 24 h. Any changes in the appearance of the samples were recorded with an 8.1 mega pixel Cyber-shot Sony camera, model DSC-H3.

## Differential Scanning Calorimetry (DSC)

The melting temperature ( $T_m$ ) and melting enthalpy ( $\Delta H_m$ ) of the films were measured using a DSC Pyris 1, Perkin Elmer (Massachusetts, USA). Temperature and heat flux were previously calibrated using indium and zinc. About 5 mg of each sample were placed in hermetically sealed aluminum pans and heated from  $-60$  to  $210$  °C at a scanning rate of  $10$  °C/min under nitrogen atmosphere. Changes of phase or state and the corresponding melting enthalpies were then determined from the melting peaks of the DSC thermograms [13]. The crystallinity percentage values of the PCL-containing samples were calculated according to the following equation [14]:

$$\text{Crystallinity (\%)} = \left( \frac{\Delta H_m}{w_{\text{PCL}} \times \Delta H_{100}} \right) \times 100 \quad (2)$$

where  $\Delta H_m$  is the experimental melting enthalpy,  $w_{\text{PCL}}$  is the PCL weight fraction and  $\Delta H_{100}$  is the melting enthalpy of 100% crystalline PCL (142 J/g) [15]. Three samples were analyzed for each film system, and the mean crystallinity percentage values  $\pm$  SD were reported.

## Scanning Electron Microscopy (SEM)

A JEOL JSM-6460 LV instrument was used to analyze the surfaces of the thermo-compressed films of each material. Prior to their analysis, the films were mounted on bronze stubs and sputter-coated (Sputter coater SPI Module, Santa Clara, CA, USA) with a thin layer of gold for 35 s.

## Atomic Force Microscopy (AFM)

An Agilent 5500 was used to obtain the topographic images of the films in the Acoustic AC Mode (AAC Mode) using silicon nitride ( $\text{Si}_3\text{N}_4$ ) tips. The tips were 2 mm long and V-shaped, with a spring constant of  $0.2 \text{ N m}^{-1}$ . They were positioned over the each sample with a cantilever oscillation frequency of 155 kHz under ambient conditions. The AFM images were taken at the center and periphery of the surface of the films exposed to the thermo-compression process. The images were then processed with PicoView image software.

## Color

The CIE- $L^*a^*b^*$  coordinates of the surfaces of the films exposed to the thermo-compression process were measured according to the standard test method (ASTM D-1925, 1995) using a Macbeth® colorimeter in reflectance mode (Color-Eye 2445 model, illuminant D65 and  $10^\circ$  observer) and standardized with a white reference plate ( $L^* = 93.52$ ,  $a^* = -0.81$  and  $b^* = 1.58$ ). Color differences ( $\Delta E$ ) were calculated according to Valencia Rodríguez [16], the whiteness index (WI) following Atarés et al. [17], and the yellowness index (YI) according to ASTM [18].

## Opacity

The opacity was determined following the method proposed by Sukhija et al. [17]. The ultraviolet (UV) and visible light barrier properties of the dried films were measured at selected wavelengths between 400 and 800 nm using a UV–Vis spectrophotometer (u-2001, Japan). Film opacity was then measured at 600 nm and calculated using the following equation given by Han and Floros [19]:

$$\text{Opacity} = A_{600}/e \quad (3)$$

where  $A_{600}$  = the absorbance at 600 nm and “ $e$ ” is the film thickness (mm).

## Statistical Analysis

The data were analyzed with an analysis of variance (ANOVA) test using OriginPro 8 (Version 8.5, Northampton, USA) software. The results of the statistical analyses were presented as mean values  $\pm$  standard deviation (SD). Differences between the mean values of the measured properties were compared using the multiple-range Tukey’s test. A significance level of 0.05 was employed.

## Results and Discussion

### Attenuated Total Reflectance Fourier Transform Infrared Spectroscopy (ATR/FTIR)

Figure 1a shows the ATR/FTIR spectra of the different films studied over the whole absorption range. A significant absorption peak at around  $3282 \text{ cm}^{-1}$  associated with the stretching of the OH groups belonging to the starch, glycerol and water, and the stretching vibration of the C–O groups was observed in all the systems studied [20]. According to Gutiérrez [1] starch-based materials

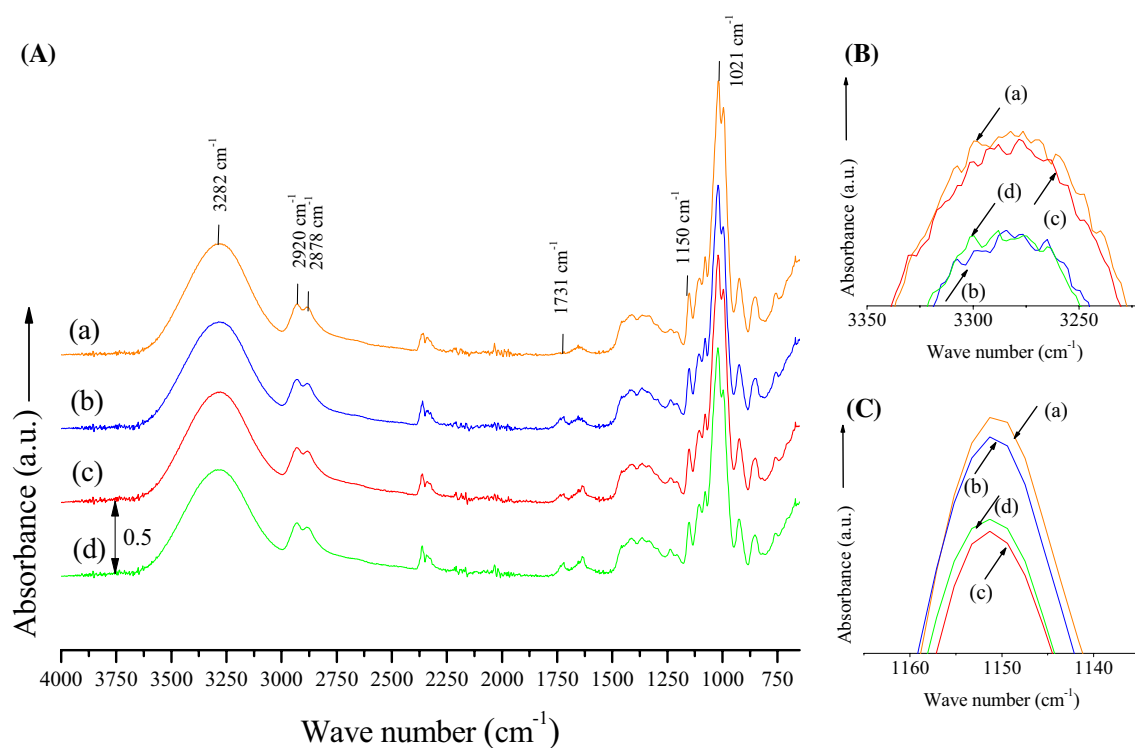


**Fig. 1** **a** FTIR spectra of the different films studied in all the absorption range. **b** FTIR spectra in the absorption range corresponding to C–O group (OH stretching) of the different films studied. **c** FTIR spectra in the absorption range between 1140 and 1160  $\text{cm}^{-1}$ . Ther-

moplastic starch (TPS) and thermoplastic flour (TPF) films: *a* native sagu starch (TPS-NSS), *b* native sagu starch/PCL blend (TPS-NSS/PCL), *c* native sagu flour (TPF-NSF) and *d* native sagu flour/PCL blend (TPF-NSF/PCL)

with a greater number of free OH groups vibrate more easily and thus tend to have wider bands with higher levels of absorbance. It can thus be inferred from Fig. 1b that the number of OH groups in each of the film formulations increased in the following order: TPS-NSS/PCL  $\approx$  TPF-NSF/PCL < TPS-NSS  $\approx$  TPF-NSF. Shi et al. [21] proposed another method to compare the number of available OH groups in these types of systems: the ratio between the band intensities at  $\sim 3300 \text{ cm}^{-1}$  ( $I_{3300}$ ) (Fig. 1b) and  $1150 \text{ cm}^{-1}$  ( $I_{1150}$ ) (Fig. 1c) ( $I_{3300}/I_{1150}$  ratio). Following this procedure, the ascending order of the number of OH groups in the film systems was: TPS-NSS/PCL (1.77) < TPS-NSS (1.80) < TPF-NSF/PCL (1.97) < TPF-NSF (2.07). Both methods produced the expected results, i.e. the PCL-containing films had fewer free OH groups associated with the starch matrix than the films without added PCL. Furthermore, the method proposed by Shi et al. [21] showed that the TPF-NSF/PCL film contained more available OH groups than the TPS-NSS/PCL film. In a previous study undertaken by our research team we demonstrated that greater phase separation occurs in the TPF-NSF/PCL film than in the TPS-NSS/PCL film [7]. We can assume, therefore, that this greater phase separation in the TPF-NSF/PCL film frees the glycerol molecules, thus

enabling the moisture adsorption from the environment and increasing the number of free OH groups. In addition, the results reported here suggest that the sagu flour-based film (TPF-NSF) is more susceptible to moisture adsorption than the sagu starch-based film (TPS-NSS), since the former has a greater number of available OH groups to adsorb moisture from the atmosphere.

The band located at  $1731 \text{ cm}^{-1}$  (Fig. 1a) in the PCL-containing films represents the C=O groups of the esters in the PCL, thus confirming their presence. Particularly, this band was more intense in the TPF-NSF/PCL film compared to the TPS-NSS/PCL film, thus demonstrating the lower PCL-flour interaction. Other peaks located at 2878 and  $2920 \text{ cm}^{-1}$  are associated with C–H stretch vibrations [22] and are characteristic of starch polymeric matrix materials; the bands observed between 1362 and  $1497 \text{ cm}^{-1}$  are assigned to C–O angular deformations [23]; and the band detected at  $\sim 1021 \text{ cm}^{-1}$  in all the films developed is associated with –C–O–C– glycosidic bonds [1].

### Determination of Film Thickness (e)

The thicknesses of the different film systems studied are shown in Table 1. According to Pérez et al. [24] and

**Table 1** Thickness ( $e$ ), density ( $\rho$ ), water activity ( $a_w$ ), color parameters and opacity of the different films

Parameter	TPS-NSS	TPS-NSS/PCL	TPF-NSF	TPF-NSF/PCL
$e$ (mm)	$1.36 \pm 0.05^b$	$1.17 \pm 0.04^a$	$1.29 \pm 0.04^b$	$1.15 \pm 0.05^a$
$\rho$ (g/cm <sup>3</sup> )	$0.75 \pm 0.07^b$	$0.61 \pm 0.05^a$	$0.68 \pm 0.04^a$	$0.66 \pm 0.03^a$
$a_w$	$0.413 \pm 0.001^a$	$0.423 \pm 0.001^b$	$0.425 \pm 0.001^b$	$0.450 \pm 0.002^c$
$L^*$	$37.30 \pm 0.01^c$	$40.78 \pm 0.02^d$	$12.72 \pm 0.02^a$	$20.74 \pm 0.02^b$
$a^*$	$0.78 \pm 0.01^b$	$-0.32 \pm 0.02^a$	$1.35 \pm 0.07^c$	$2.57 \pm 0.04^d$
$b^*$	$8.03 \pm 0.01^d$	$2.58 \pm 0.03^b$	$1.27 \pm 0.08^a$	$3.30 \pm 0.05^c$
Color difference ( $\Delta E$ )	$56.63 \pm 0.01^b$	$52.78 \pm 0.02^a$	$80.85 \pm 0.02^d$	$72.90 \pm 0.02^c$
Whiteness index (WI)	$36.78 \pm 0.01^c$	$40.72 \pm 0.02^d$	$12.70 \pm 0.02^a$	$20.63 \pm 0.02^b$
Yellow index (YI)	$30.88 \pm 0.04^d$	$9.0 \pm 0.1^a$	$13.3 \pm 0.5^b$	$24.4 \pm 0.2^c$
Opacity	$1.23 \pm 0.01^a$	$1.45 \pm 0.01^c$	$1.34 \pm 0.01^b$	$1.52 \pm 0.01^d$

Equal letters in the same row indicate no statistically significant differences ( $p \leq 0.05$ ). Thermoplastic starch (TPS) and thermoplastic flour (TPF) films: native sagu starch (TPS-NSS), native sagu starch/PCL blend (TPS-NSS/PCL), native sagu flour (TPF-NSF) and native sagu flour/PCL blend (TPF-NSF/PCL)

Gutiérrez et al. [25] a significant increase in the thickness of starch-based films is indicative of a greater number of stronger chemical interactions (mainly hydrogen bonding) among the constituents of the films. Films without added PCL (TPS-NSS and TPF-NSF) were significantly ( $p \leq 0.05$ ) thicker than the PCL-containing films (TPS-NSS/PCL and TPF-NSF/PCL). These results thus predict that fewer interactions among the film components took place in the films with added PCL. This would be in line with Gutiérrez and Alvarez [7] who demonstrated that the addition of PCL to these film systems led to phase separation.

No statistically significant differences ( $p \geq 0.05$ ) were observed between the PCL-containing systems (TPS-NSS/PCL and TPF-NSF/PCL), or between the films without added PCL (TPS-NSS and TPF-NSF).

### Density ( $\rho$ )

The density values of the films studied are shown in Table 1. Gutiérrez [1] and Pelissari et al. [26] suggested that the density of starch-based films depends on the type of polymer structure, the molecular weight of the polymer, and the chemical interactions that occur within the material. The TPS-NSS film was the densest ( $0.75 \text{ g/cm}^3$ ) of the films analyzed suggesting that the strongest chemical interactions occurred among its constituents. Higher density values have, however, been reported by Pelissari et al. [26] for banana starch films ( $1.34 \text{ g/cm}^3$ ) and by Müller et al. [27] for cassava starch films ( $2.41 \text{ g/cm}^3$ ), which in both cases were obtained by the casting methodology. It is interesting that the trend observed here, namely that the sagu flour film (TPF-NSF,  $0.58 \text{ g/cm}^3$ ) was less dense than the sagu starch film (TPS-NSS,  $0.75 \text{ g/cm}^3$ ), is the same as that reported by Pelissari et al. [26] whereby the banana flour film ( $1.18 \text{ g/cm}^3$ ) was also less dense than the banana starch film ( $1.34 \text{ g/cm}^3$ ). Finally, there was no

significant difference ( $p \geq 0.05$ ) between the densities of the PCL-containing films (TPS-NSS/PCL,  $0.61 \pm 0.05 \text{ g/cm}^3$  and TPF-NSF/PCL,  $0.66 \pm 0.03 \text{ g/cm}^3$ ).

### Water Activity ( $a_w$ )

The water activity of the films is reported in Table 1. The water activity of a material is associated with free water or water available within it. The PCL-containing films (TPS-NSS/PCL and TPF-NSF/PCL) showed higher water activity values than the films without added PCL (TPS-NSS and TPF-NSF). Taking into account that these PCL-containing systems also presented phase separation [7], we can surmise that the phase separation in the PCL-containing films resulted in the glycerol being released from the matrix. This free glycerol adsorbed moisture from the environment, thus increasing the water activity values in the PCL-containing systems. This was more noticeable for the TPF-NSF/PCL film than the TPS-NSS/PCL film, confirming the greater phase separation observed by Gutiérrez and Alvarez [7] for the former as compared to the latter. This is in line with the results of the analysis of the ATR/FTIR spectra (Sect. 3.1).

In addition, the sagu flour film (TPS-NSS) showed a higher water activity value than the sagu starch film (TPF-NSF). Thus, the flour based film is more susceptible to moisture adsorption than the starch film. This agrees with the results for the banana flour film compared to the banana starch film reported by Pelissari et al. [26].

Overall, the sagu starch film showed the lowest water activity value of all the systems tested (TPS-NSS, 0.413). Based on this result and the others analyzed above, we can conclude that the hydrogen bonding interactions between the constituents of the TPS-NSS film (sagu starch-glycerol) are stronger than those of the other films developed.



It is worth noting that despite the differences between the water activity values of the different films obtained, they were all too low for microbiological growth [28].

### Stability in Acidic or Alkaline Solutions

Figure 2 shows the digital photographs of the films immersed in acid (pH 1), neutral (pH 7) and alkaline (pH 13) media for 24 h. All the films were stable (unchanged) in the acid and the neutral media, and could therefore be successfully used under these conditions. Similar results were reported by Gutiérrez et al. [29] for films prepared from native and phosphated plantain flour. In contrast, immersion in the alkaline medium produced alterations in all the films tested. According to Gutiérrez et al. [30] the dissolution and disintegration of starch films under alkaline conditions could be due to reactions between the sodium hydroxide and the hydroxyl groups of the starch molecules. This reduces and destroys the intermolecular hydrogen bonding interactions between the starch macromolecules and the glycerol, resulting in swelling and starch gelatinization [1]. It can be seen from Fig. 2 that the TPS-NSS film was the most stable in the alkaline medium although some slight swelling was observed. From the previous discussions, this means that there must be more and stronger hydrogen bonding interactions between the starch and glycerol in the TPS-NSS film system. These stronger interactions resist being broken up by the sodium hydroxide thus making the TPS-NSS film more stable under alkaline conditions. In contrast, the PCL-containing films (TPS-NSS/PCL and TPF-NSF/PCL) suffered disruption of their matrices. It is possible that the

phase separation reported for these systems enabled sodium hydroxide to penetrate more easily into the matrices thus decreasing their stability. Finally, it is worth noting that the sagu starch-based film (TPS-NSS) was more stable than the sagu flour-based film (TPF-NSF). This is likely due to the lower number of available OH groups in the TPS-NSS film compared to the TPF-NSF film (see Sect. 3.1) which probably limits interactions between the sodium hydroxide and the starch matrix in this system.

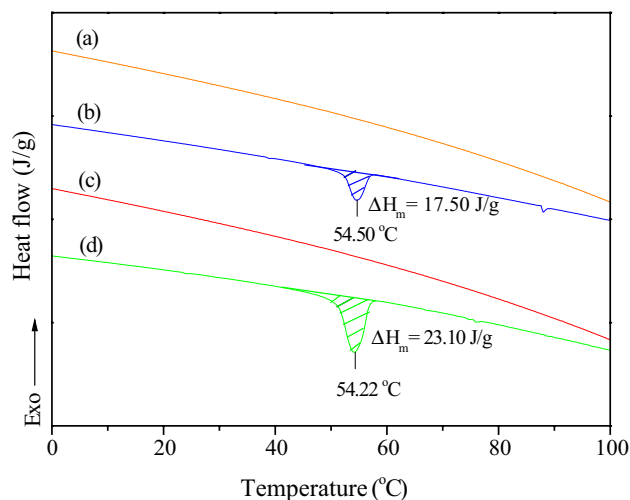
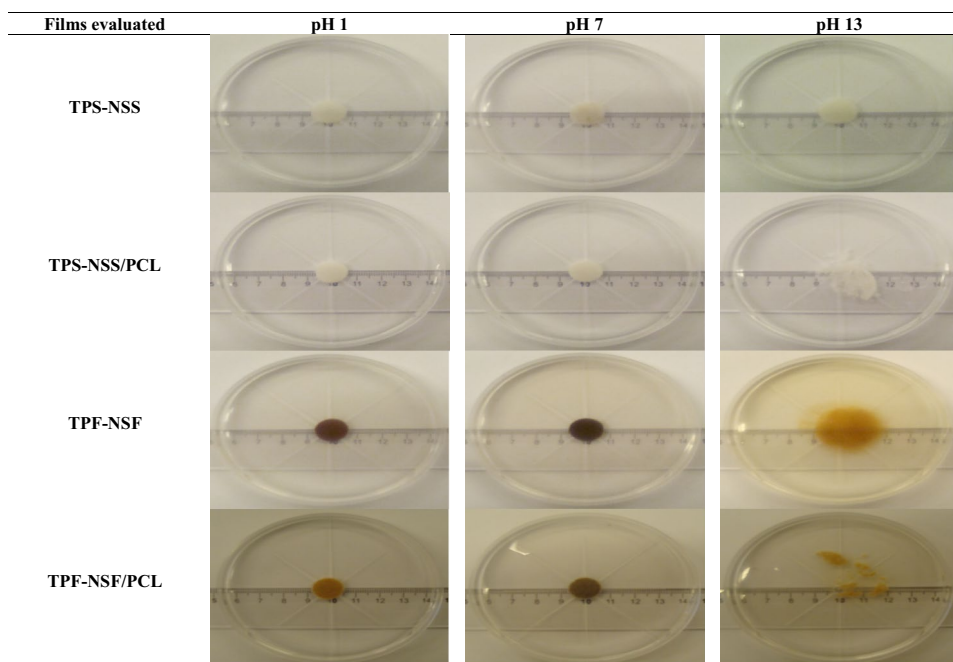


**Fig. 3** Heating thermograms of the films based on: *a* native sagu starch (TPS-NSS), *b* native sagu starch/PCL blend (TPS-NSS/PCL), *c* native sagu flour (TPF-NSF) and *d* native sagu flour/PCL blend (TPF-NSF/PCL)

**Fig. 2** Digital photographs of the films immersed in acid, neutral and alkaline medium after 24 h. Thermoplastic starch (TPS) and thermoplastic flour (TPF) films: Native sagu starch (TPS-NSS), native sagu starch/PCL blend (TPS-NSS/PCL), native sagu flour (TPF-NSF) and native sagu flour/PCL blend (TPF-NSF/PCL)



## Differential Scanning Calorimetry (DSC)

The DSC curves for the developed films are shown in Fig. 3. It should be noted that the glass transition temperature ( $T_g$ ) of these materials were not evident, i.e. data related to the analysis of the amorphous phase by DSC cannot be discussed in this study. This fact is possibly related by the domain of the crystalline phase over the amorphous phase. For this reason, the discussion in this section will be directed to the study of the crystalline phase of the materials developed. The melting temperature ( $T_m$ ) of PCL is in the range of 55–65 °C [31]. The endothermic peaks at 54 °C in the PCL-containing films were thus consistent with the  $T_m$  of the crystalline fraction of the PCL. The melting temperatures of the two PCL-containing films were not significantly different ( $p \geq 0.05$ ). We can thus conclude that either sagu starch or flour can be used in blends with PCL without affecting this parameter. Similar behavior was reported by Ortega-Toro et al. [5] for films prepared from starch/PCL blends in varying proportions.

Higher melting enthalpy ( $\Delta H_m$ ) values have been correlated with the crystalline fraction of polymers [32]. The crystallinity percentages of the PCL-containing films were calculated from the  $\Delta H_m$  values (Fig. 3) following the methodology proposed by Merino et al. [12], and were 20.5 and 27.1% for TPS-NSS/PCL and TPF-NSF/PCL

films, respectively. In contrast, the films without added PCL were mainly amorphous (crystallinity percentage values < 1%).

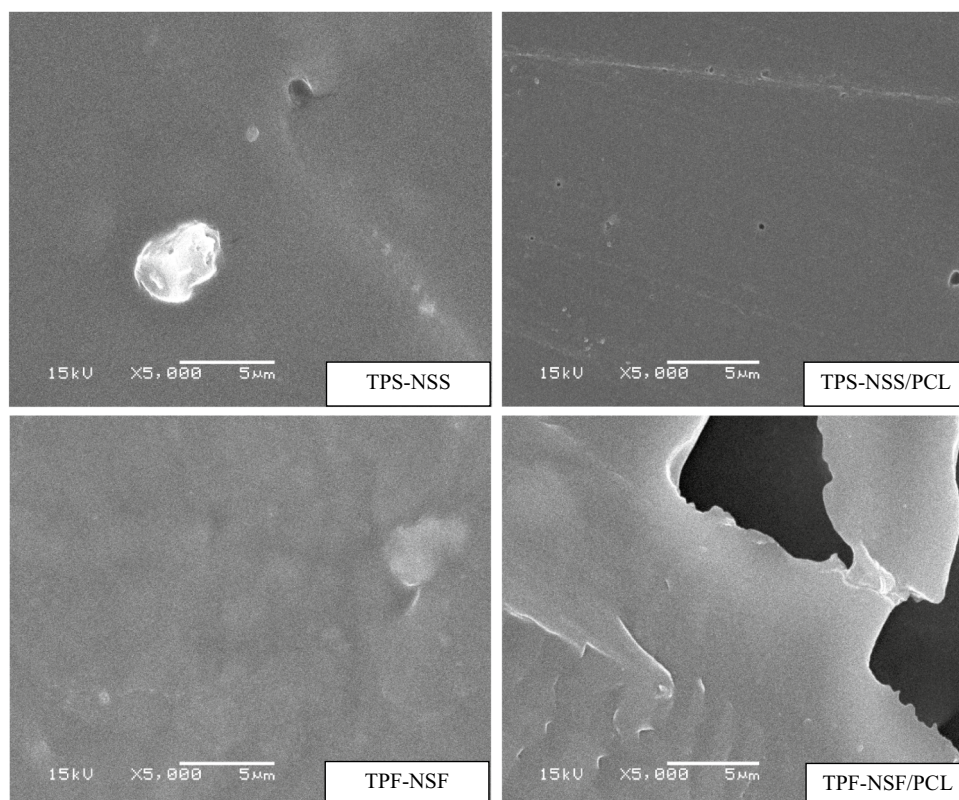
The TPF-NSF/PCL film showed a 1.3-fold increase in both the  $\Delta H_m$  and the crystallinity percentage compared to the TPS-NSS/PCL film. This despite having the same starchy matrix:PCL ratio. Possibly, the greater phase separation that occurred in the TPF-NSF/PCL film enabled the PCL crystalline fraction to be expressed more easily than in the TPF-NSF/PCL film where the stronger sagu starch-PCL interactions inhibited the expression of this fraction.

## Scanning Electron Microscopy (SEM)

The SEM micrographs of the surfaces of the different films studied are shown in Fig. 4. Starch granules were not observed on any of the samples indicating that the starch was gelatinized and plasticized successfully under the processing conditions used, thus giving rise to the formation of thermoplastic starch.

It can also be observed that the TPS-NSS and TPF-NSF films produced were non-porous and compact. In particular, a distinct grainy patch was observed on the surface of the TPS-NSS film. Gutiérrez and Alvarez [7] previously reported that sagu starch has a greater tendency to retrogradation than sagu flour. The grainy patch on the surface of the TPS-NSS film could thus be associated with the

**Fig. 4** SEM micrographs of the surface of the films based on: native sagu starch (TPS-NSS), native sagu starch/PCL blend (TPS-NSS/PCL), native sagu flour (TPF-NSF) and native sagu flour/PCL blend (TPF-NSF/PCL). At 5 k $\times$  of magnification



retrogradation process. Similar observations were made by Gutiérrez et al. [29] for films based on native and phosphated plantain flour.

The PCL-containing films exhibited poor interfacial adhesion because of the different polymer polarities present. Similar morphological images were reported by Ortega-Toro et al. [5] for films made from varying starch:PCL ratios. It should be noted that the TPF-NSF/

PCL film was more porous than the TPS-NSS/PCL film, thus demonstrating the greater polarity difference between the sagu flour and PCL compared to that of the sagu starch and PCL. To summarize, we can say that the difference in polarity between the polymers used is directly proportional to the degree of phase separation of the resulting polymer matrix. This leads to the production of more porous

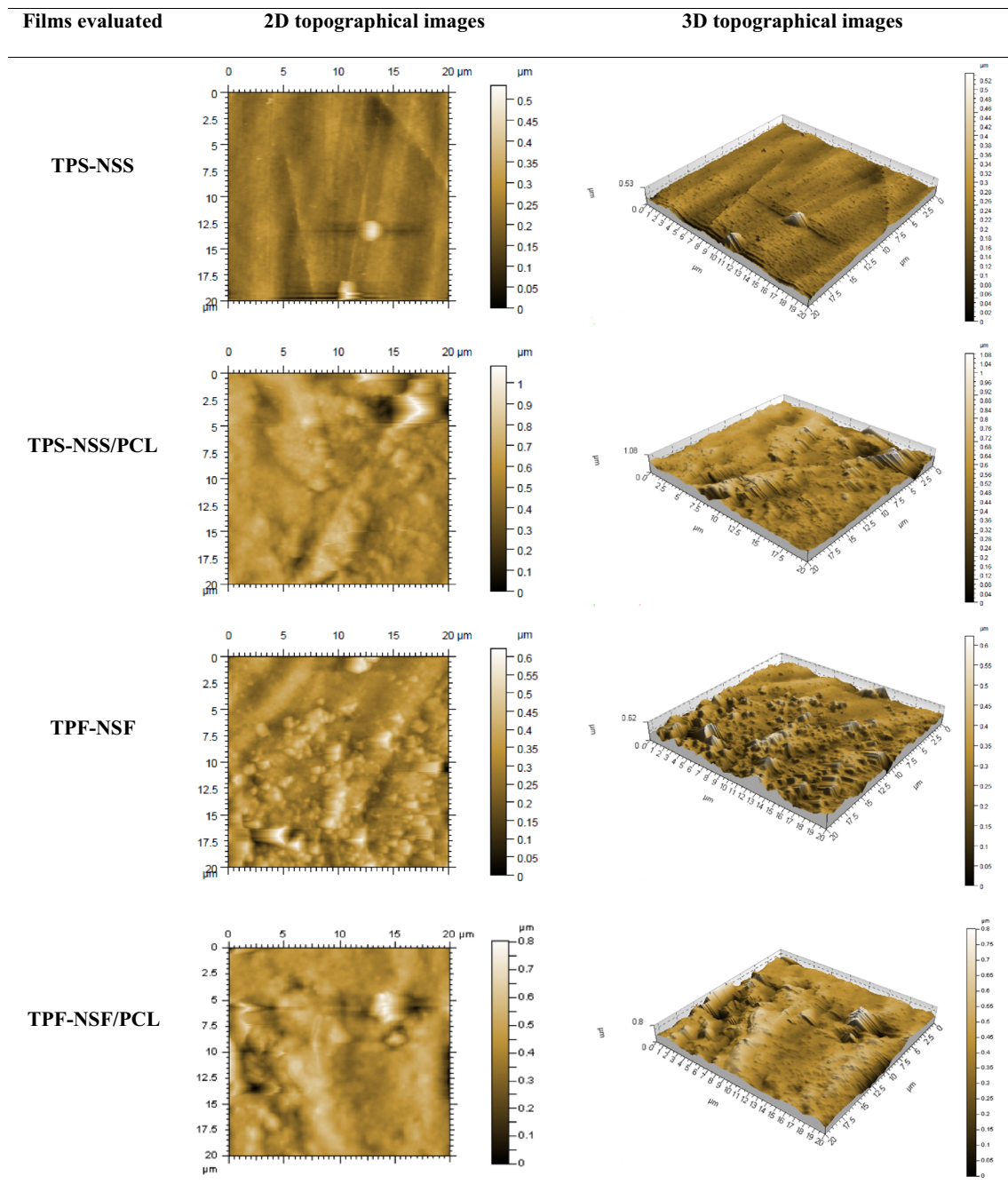


**Fig. 5** AFM images of the surface of the films based on: native sagu starch (TPS-NSS), native sagu starch/PCL blend (TPS-NSS/PCL), native sagu flour (TPF-NSF) and native sagu flour/PCL blend (TPF-NSF/PCL)



materials with poor interfacial adhesion. This agrees with the rest of the results discussed above.

### Atomic Force Microscopy (AFM)

The 2D and 3D topographical images of the different films analyzed by AFM are shown in Fig. 5. The AFM surface topographical images are consistent with the SEM images for all the films studied. The AFM images were also used to determine average roughness ( $R_a$ ) as follows (in order of ascension): 140 nm (TPS-NSS) < 200 nm (TPF-NSF) < 300 nm (TPS-NSS/PCL) < 350 nm (TPF-NSF/PCL). The TPS-NSS film was thus the smoothest and softest of the films studied. Apparently, stronger hydrogen bond interactions between the sagu starch and glycerol led to films with lower  $R_a$  values. The PCL-containing films had more rugged surfaces than the films without added PCL, probably due to the poorer surface adhesion between the polymers. Similar results were reported by Ortega-Toro et al. [5] for films prepared from varying starch:PCL ratios. The TPF-NSF/PCL film showed the highest  $R_a$  value. The greater phase separation recorded for this film system could be linked to this surface morphology. The sagu flour-based film (TPF-NSF) had a greater roughness than the sagu starch-based film (TPS-NSS) which was possibly related to the fiber content (cellulosic material) found in sagu flour. Higher  $R_a$  values have been reported by López et al. [33] for corn thermoplastic starch films containing agro-industrial cellulosic residues compared to films with aggregate residues.

### Color

The results of the color parameters of the films are shown in Table 1. The  $L^*$  values suggest that the TPF-NSF film was the darkest material. In addition, the PCL-containing films (TPS-NSS/PCL and TPF-NSF/PCL) were whiter than films without added PCL (TPS-NSS and TPF-NSF). The values of the whiteness index (WI) and the  $L^*$  thus reinforce each other.

Negative  $a^*$  values indicate greener materials, and positive  $a^*$  values redder ones. The TPS-NSS/PCL film tended towards green, whilst the other films tended towards red. The TPF-NSF/PCL film was the reddest of the systems examined.

Positive  $b^*$  values indicate a tendency towards yellow thus all the materials developed were yellowish (Table 1) particularly the TPS-NSS film. The highest values of both  $b^*$  and the yellow index (YI) found for the TPS-NSS film fit well with the previous discussion.

### Opacity

The opacity values of the different systems studied are shown in Table 1. The films developed had the following ascending order of opacity: TPS-NSS (1.23) < TPF-NSF (1.34) < TPS-NSS/PCL (1.45) < TPF-NSF/PCL (1.52). A positive relationship between opacity and the  $R_a$  values was observed. It can thus be presumed that greater surface roughness prevents the effective transmission of UV radiation through the material, i.e. UV radiation is adsorbed by imperfections on the surface of the material, thus increasing the opacity. Gutiérrez and González [34] reached a similar conclusion in other research papers.

It is worth noting that the PCL-containing films were more opaque than those without PCL. A similar trend was observed by Ortega-Toro et al. [5] for films prepared from varying starch:PCL ratios. According to Sukhija et al. [35] more opaque films may be used to protect compounds susceptible to oxidative degradation catalyzed by UV radiation. The PCL-containing films (TPS-NSS/PCL and TPF-NSF/PCL) examined here could potentially be employed to protect foods in this way.

It should also be noted that higher percentages of crystallinity were positively correlated with film opacity. This may be because crystalline sites within the polymeric material could also disperse light resulting in the development of more opaque, i.e. less transparent, materials. It seems then that the degree of opacity depends not only on the surface characteristics of the material, but also on the crystalline sites within it. Thus, the opacity of the films depends fundamentally on the chemical interactions that occur within them.

### Conclusions

Two non-conventional starchy matrices (sagu starch and flour) were evaluated as potential biological macromolecules for the development of composite materials. Biological macromolecule composite films were prepared from sagu starch and flour/poly( $\epsilon$ -caprolactone) blends in order to reduce the water sensitivity common to starch-based films. Nonetheless, a marked phase separation in these systems led to conflicting results. Unfortunately the flour-based films proved to be more susceptible to moisture adsorption than the starch-based ones. This is regrettable, since flour-based films could be more cost-effective at an industrial scale. Finally, surface imperfections as well as crystalline sites within the polymeric materials gave rise to more opaque films.

**Acknowledgements** The authors would like to thank the Consejo Nacional de Investigaciones Científicas y Técnicas (CONICET)

(Postdoctoral fellowship internal PDTs-Resolution 2417), Universidad Nacional de Mar del Plata (UNMdP) for financial support. Dr. Mirian Carmona-Rodríguez for their valuable contribution. Thanks also to the Institute of Food Science and Technology (ICTA) of the Central University of Venezuela (UCV), especially Jusneydy Suniaga, for managing the purchase of the rhizomes from the Venezuelan Amazon, as well as obtaining isolated starch and flour, and the determination of water activity and color parameters of the films. Many thanks also to Dr. Gema González and M.Sc. Antonio Monsalve of Venezuelan Institute for Scientific Research (IVIC) for allowing the M.Sc. Keltia Álvarez to carry out the acquisition of AFM images in her laboratory.

## Compliance with Ethical Standards

**Conflicts of interest** The author declares no conflict of interest.

## References

- Gutiérrez TJ (2017) Effects of exposure to pulsed light on molecular aspects of edible films made from cassava and taro starch. *Innov Food Sci Emerg Technol* 41:387–396. <https://doi.org/10.1016/j.ifset.2017.04.014>
- Gutiérrez TJ (2017) Surface and nutraceutical properties of edible films made from starchy sources with and without added blackberry pulp. *Carbohydr Polym* 165:169–179. <https://doi.org/10.1016/j.carbpol.2017.02.016>
- Fabra MJ, Lopez-Rubio A, Lagaron JM (2013) High barrier polyhydroxycalcaneate food packaging film by means of nanostructured electrospun interlayers of zein. *Food Hydrocoll* 32:106–114. <https://doi.org/10.1016/j.foodhyd.2012.12.007>
- Ortega-Toro R, Morey I, Talens P, Chiralt A (2015) Active bilayer films of thermoplastic starch and polycaprolactone obtained by compression molding. *Carbohydr Polym* 127:282–290. <https://doi.org/10.1016/j.carbpol.2015.03.080>
- Ortega-Toro R, Contreras J, Talens P, Chiralt A (2015) Physical and structural properties and thermal behaviour of starch-poly( $\epsilon$ -caprolactone) blend films for food packaging. *Shelf Life* 5:10–20. <https://doi.org/10.1016/j.fpsl.2015.04.001>
- Kweon D-K, Kawasaki N, Nakayama A, Aiba S (2004) Preparation and characterization of starch/polycaprolactone blend. *J Appl Polym Sci* 92:1716–1723. <https://doi.org/10.1002/app.20130>
- Gutiérrez TJ, Alvarez VA (2017) Films made by blending poly( $\epsilon$ -caprolactone) with starch and flour from sagu rhizome grown at the venezuelan amazons. *J Polym Environ* 25:701–716. <https://doi.org/10.1007/s10924-016-0861-9>
- Gutiérrez TJ, Alvarez VA (2017) Cellulosic materials as natural fillers in starch-containing matrix-based films: a review. *Polym Bull* 74:2401–2430. <https://doi.org/10.1007/s00289-016-1814-0>
- Pérez E, Bahnsen YA, Breene WM (1993) A simple laboratory scale method for isolation of amaranth starch. *Starch-Stärke* 45:211–214. <https://doi.org/10.1002/star.19930450605>
- Pacheco E (2001) Evaluación nutricional de sopas deshidratadas a base de harina de plátano verde. Digestibilidad in vitro de almidón. *Acta Científica Venez* 52:278–282. <http://acta.ivic.gob.ve/52-4/articulo6.pdf>
- Mollega Mainsard IP (2008) Caracterización y biodegradación de mezclas de policaprolactona y poliláctico con almidón de yuca. Universidad Simón Bolívar. <http://159.90.80.55/tesis/000144538.pdf>
- Maliger RB, Halley PJ (2014) Reactive extrusion for thermoplastic starch-polymer blends. In: Halley PJ, Avérous LR (eds) *Starch polymers*. Elsevier, Burlington, pp 291–317 <https://doi.org/10.1016/B978-0-444-53730-0.00030-0>
- Biliaderis CG, Lazaridou A, Arvanitoyannis I (1999) Glass transition and physical properties of polyol-plasticised pullulan–starch blends at low moisture. *Carbohydr Polym* 40:29–47. [https://doi.org/10.1016/S0144-8617\(99\)00026-0](https://doi.org/10.1016/S0144-8617(99)00026-0)
- Merino D, Ludueña LN, Alvarez VA (2018) Dissimilar tendencies of innovative green clay organo-modifier on the final properties of poly( $\epsilon$ -caprolactone) based nanocomposites. *J Polym Environ* 26(2):716–727. <https://doi.org/10.1007/s10924-017-0994-5>
- H. Tsuji, T. Ishizaka, Porous biodegradable polyesters, 3. preparation of porous poly( $\epsilon$ -caprolactone) films from blends by selective enzymatic removal of poly(L-lactide), *Macromol Biosci* 1 (2001) 59–65
- Valencia MT, Rodríguez (2001) Efecto del tratamiento de preservación por depresión e la actividad acuosa en la calidad del alga. Universidad de Buenos Aires, Buenos Aires
- Atarés L, Bonilla J, Chiralt A (2010) Characterization of sodium caseinate-based edible films incorporated with cinnamon or ginger essential oils. *J Food Eng* 100:678–687. <https://doi.org/10.1016/j.jfoodeng.2010.05.018>
- ASTM D1925-70 (1988) Test method for yellowness index of plastics. <http://www.astm.org/Standards/D1925.htm>
- Han JH, Floros JD (1997) Casting antimicrobial packaging films and measuring their physical properties and antimicrobial activity. *J Plast Film Sheeting* 13:287–298. <https://doi.org/10.1177/875608799701300405>
- Pereira VA, de Arruda INQ, Stefani R (2015) Active chitosan/PVA films with anthocyanins from *Brassica oleraceae* (Red Cabbage) as time–temperature indicators for application in intelligent food packaging. *Food Hydrocoll* 43:180–188. <https://doi.org/10.1016/j.foodhyd.2014.05.014>
- Shi R, Zhang Z, Liu Q, Han Y, Zhang L, Chen D, Tian W (2007) Characterization of citric acid/glycerol co-plasticized thermoplastic starch prepared by melt blending. *Carbohydr Polym* 69:748–755. <https://doi.org/10.1016/j.carbpol.2007.02.010>
- Mathew S, Brahmakumar M, Abraham TE (2006) Microstructural imaging and characterization of the mechanical, chemical, thermal, and swelling properties of starch–chitosan blend films. *Biopolymers* 82:176–187. <https://doi.org/10.1002/bip.20480>
- Batista Reis LC, Oliveira de Souza C, Alves da Silva JB, Martins AC, Larroza Nunes I, Druzian JI (2015) Active biocomposites of cassava starch: the effect of yerba mate extract and mango pulp as antioxidant additives on the properties and the stability of a packaged product. *Food Bioprod Process* 94:382–391. <https://doi.org/10.1016/j.fbp.2014.05.004>
- Pérez E, Segovia X, Tapia MS, Schroeder M (2012) Native and cross-linked modified *Dioscorea trifida* (cush-cush yam) starches as bio-matrices for edible films. *J Cell Plast* 48:545–556. <https://doi.org/10.1177/0021955X12445603>
- Gutiérrez TJ, Tapia MS, Pérez E, Famá L (2015) Structural and mechanical properties of edible films made from native and modified cush-cush yam and cassava starch. *Food Hydrocoll* 45:211–217. <https://doi.org/10.1016/j.foodhyd.2014.11.017>
- Pelissari FM, Andrade-Mahecha MM, PJ do A Sobral, Menegalli FC (2013) Comparative study on the properties of flour and starch films of plantain bananas (*Musa paradisiaca*). *Food Hydrocoll* 30:681–690. <https://doi.org/10.1016/j.foodhyd.2012.08.007>
- Müller CMO, Laurindo JB, Yamashita F (2009) Effect of cellulose fibers addition on the mechanical properties and water vapor barrier of starch-based films. *Food Hydrocoll* 23:1328–1333. <https://doi.org/10.1016/j.foodhyd.2008.09.002>
- Jay JM (1995) Intrinsic and extrinsic parameters of foods that affect microbial growth. In: Jay JM (ed) *Modern food microbiol*. 5th ed. Springer, Boston, pp 38–66. [https://doi.org/10.1007/978-1-4615-7476-7\\_3](https://doi.org/10.1007/978-1-4615-7476-7_3)
- Gutiérrez TJ, Suniaga J, Monsalve A, García NL (2016) Influence of beet flour on the relationship surface-properties of edible and

- intelligent films made from native and modified plantain flour. *Food Hydrocoll* 54:234–244. <https://doi.org/10.1016/j.foodhyd.2015.10.012>
30. Gutiérrez TJ, Morales NJ, Pérez E, Tapia MS, Famá L (2015) Physico-chemical properties of edible films derived from native and phosphated cush-cush yam and cassava starches. *Food Packag Shelf Life* 3:1–8. <https://doi.org/10.1016/j.fpsl.2014.09.002>
31. Labet M, Thielemans W (2009) Synthesis of polycaprolactone: a review. *Chem Soc Rev* 38:3484–3504. <https://doi.org/10.1039/B820162P>
32. Mitrus M (2005) Glass transition temperature of thermoplastic starches. *Int Agrophys* 19:237–241. [http://www.old.international-agrophysics.org/artykuly/international\\_agrophysics/IntAgr\\_2005\\_19\\_3\\_237.pdf](http://www.old.international-agrophysics.org/artykuly/international_agrophysics/IntAgr_2005_19_3_237.pdf)
33. López OV, Versino F, Villar MA, García MA (2015) Agro-industrial residue from starch extraction of *Pachyrhizus ahipa* as filler of thermoplastic corn starch films. *Carbohydr Polym* 134:324–332. <https://doi.org/10.1016/j.carbpol.2015.07.081>
34. Gutiérrez TJ, González G (2016) Effects of exposure to pulsed light on surface and structural properties of edible films made from cassava and taro starch. *Food Bioprocess Technol* 9:1812–1824. <https://doi.org/10.1007/s11947-016-1765-3>
35. Sukhija S, Singh S, Riar CS (2016) Analyzing the effect of whey protein concentrate and psyllium husk on various characteristics of biodegradable film from lotus (*Nelumbo nucifera*) rhizome starch. *Food Hydrocoll* 60:128–137. <https://doi.org/10.1016/j.foodhyd.2016.03.023>